

## Surface Dangling Bond Effect on Magnetic Property of Mn-doped ZnO Nanowires

N. Tsogbadrakh<sup>1,2</sup>, Eun-Ae Choi<sup>1</sup>, Woo-Jin Lee<sup>1</sup>, K. J. Chang<sup>1</sup>

<sup>1</sup>Department of Physics, Korea Advanced Institute of Science and Technology (KAIST), Daejeon 305-701, Republic of Korea

<sup>2</sup>Department of Theoretical and Experimental Physics, School of Physics and Electronics, National University of Mongolia, University Street 1, Ulaanbaatar-210646, Mongolia

\*E-mail: Tsogbadrakh@num.edu.mn

We investigate the magnetic properties of Mn-doped ZnO nanowires (NWs) using the local spin density approximation (LSDA) and the LSDA+ $U$  approach, where  $U$  represents the on-site Coulomb interaction. In carrier-free (Zn,Mn)O NWs, the majority Mn  $t_a$  states are fully occupied, leading to an antiferromagnetic ground state. We examine the effect of additional  $p$ -type doping on the ferromagnetism by considering surface O dangling bonds. Localized hole carriers are generated in the majority  $t_a$  states and promote a ferromagnetic ordering via double exchange interactions, similar to the trend of bulk (Zn,Mn)O. The ferromagnetic coupling tends to increase with increasing of the hole carrier density.

**Keywords:** Diluted magnetic semiconductors, ZnO, Nanowire, LSDA+ $U$

### 1. INTRODUCTION

Diluted magnetic semiconductors (DMSs) have been considered as the promising materials for spintronic devices where both spin and charge of electrons are utilized.<sup>1</sup> To develop DMS devices, it is essential to fabricate a ferromagnetic semiconductor with the Curie temperature above room temperature. Since room-temperature ferromagnetism was theoretically predicted to exist in wide-gap semiconductors,<sup>2</sup> extensive studies have been performed for GaN and ZnO doped with transition metal (TM) ions. Especially, ZnO has attracted growing interest due to its superior material properties<sup>3,4</sup> such as transparent, semiconducting, piezoelectric, and ferromagnetic in TM-doped samples. In Mn-doped bulk ZnO, quite diverse magnetic phases have been observed, such as paramagnetic,<sup>5</sup> spin-glass,<sup>6</sup> and ferromagnetic (FM).<sup>7-11</sup> Several models have been proposed to explain the magnetic coupling between the TM ions, including Zener/RKKY, superexchange, and double exchange mechanisms. However, the origin of the ferromagnetism is still under debate. A carrier-mediated ferromagnetism was first proposed by Dietl *et al.*, using the Zener model.<sup>2</sup> From the electronic structure calculations for Mn-doped ZnO, it was suggested that bulk (Zn,Mn)O becomes ferromagnetic when the majority  $t_a$  states of the Mn ions are partially occupied.<sup>12</sup> The details of the carrier-mediated ferromagnetism were later discussed, based on level repulsions between the Mn  $d$  orbitals and the host  $p$  orbitals.<sup>13,14</sup> For bulk (Zn,Mn)O, previous first-principles density functional calculations showed that ferromagnetism can be induced by additional  $p$ -type doping using N and Li acceptors,<sup>15-21</sup> while an antiferromagnetic (AFM)

ordering is more favorable in undoped and  $n$ -type samples. The magnetic properties of bulk (Zn,Mn)O were also shown to be very sensitive to structural defects, especially Zn vacancies which enhance the ferromagnetic coupling.<sup>19-23</sup>

The electronic properties of nanoscale DMSs are strongly affected by the quantum confinement effect and large surface-to-volume ratios. Thus, the magnetic coupling between TM ions in low-dimensional systems may be distinctively different from that of bulk materials. Experimentally, the magnetic properties of Mn-doped ZnO NWs have been controversial, exhibiting paramagnetic<sup>24-25</sup> and ferromagnetic phases.<sup>26-28</sup> In ferromagnetic (Zn,Mn)O NWs, the Curie temperature strongly depends on growth conditions and incorporation of native defects, ranging from 44 to 440 K. Compared with bulk (Zn,Mn)O, there have been less theoretical studies for the magnetic properties of (Zn,Mn)O NWs. In recent theoretical calculations, (Zn,Mn)O NWs were shown to favor the FM state if Zn vacancies are introduced, while they are antiferromagnetic unless additional carriers are incorporated.<sup>29</sup> However, this study was relied on the generalized gradient approximation within the density functional theory, in which the effect of strong on-site Coulomb interaction  $U$  on the ferromagnetism was neglected. In TM-free ZnO NWs, other calculations showed that Zn vacancies alone can induce a FM ordering.<sup>30</sup>

In this paper we investigate the magnetic properties of Mn-doped ZnO nanowires and the effect of additional hole doping on ferromagnetism through first-principles density functional calculations. In defect-free (Zn,Mn)O NWs, the AFM state is found to be the ground state, similar to bulk (Zn,Mn)O. To introduce

additional hole carriers, we consider the surface O dangling bond effect. We show that the ferromagnetic coupling between the Mn ions is promoted by the localized holes in the majority Mn  $t_a$  states.

## II. CALCULATION METHOD

Our calculations are performed using the local spin density approximation (LSDA) and the LSDA+ $U$  approach, where  $U$  represents the on-site Coulomb repulsion on the localized orbitals of metal ions. We use the projector augmented wave (PAW) potentials, as implemented in the VASP code.<sup>31</sup> The wave functions are expanded in plane waves up to a kinetic energy cutoff of 400 eV. In bulk (Zn,Mn)O, we use a  $3 \times 3 \times 2$  supercell containing 96 host atoms in the wurtzite structure. In wire structures with the orientation along the [0001] direction, we use a supercell containing 96 host atoms, which corresponds to two unit cells along the wire axis, and include a vacuum region of 10 Å to avoid interactions between neighboring supercells. The summation of charge densities is done using the special  $k$ -points generated by the  $2 \times 2 \times 3$  and  $1 \times 1 \times 6$  Monkhorst-Pack meshes<sup>32</sup> for the supercell geometries of bulk and nanowire systems, respectively. The ionic positions are fully relaxed until the residual forces are less than 0.05 eV/Å. We consider ZnO NWs with the diameter of about 1 nm, in which the surface Zn and O atoms are passivated by pseudo-H atoms with 1.5 and 0.5 electrons, respectively (Fig. 1). We optimize the lattice parameters and find that the diameter decreases by 3% whereas the length increases by 2%, as compared to the unrelaxed wire.

## III. RESULTS AND DISCUSSION

In bulk ZnO, it is known that the localized Zn  $3d$  bands calculated within the LSDA are too high in energy, increasing the  $p$ - $d$  coupling between the Zn  $3d$  and O  $2p$  orbitals. Similarly, the Mn  $3d$  impurity levels are overestimated in Mn-doped ZnO, with the majority  $t_a$  states lying near the conduction band edge. In the LSDA+ $U$  approach, using the parameters  $U = 8.5$  and 4.0 eV for the Zn and Mn ions, respectively, we obtain the positions of the Zn and Mn  $3d$  bands in good agreement with experiments<sup>33,34</sup> and other theoretical calculations.<sup>20,23</sup> The majority  $t_a$  states shift down and are located just above the valence band maximum (VBM), while the nonbonding  $e_g$  states lying in the band gap in the LSDA move into the valence band. As the Mn  $3d$  levels are close to the VBM, the coupling between the Mn

$3d$  and O  $2p$  orbitals is enhanced. In the H-passivated nanowire, the LSDA+ $U$  band gap is calculated to be 3.37 eV, as compared to the bulk value of 1.68 eV.

Recent experiments showed that doped Mn ions in ZnO NWs mostly occupy the substitutional Zn sites, incorporating into the volume lattice rather than at the surface.<sup>35,36</sup> We examine the stable position of a single Mn ion by considering three different Zn sites, which are located in the core, subsurface, and surface regions in the passivated nanowire (Fig. 1). The energy of the substitutional Mn increases by 0.12 eV per Mn ion as going from the core site to the surface site, consistent with previous theoretical calculations and experiments.<sup>29,36</sup> The stability of the Mn ion in the bulk-like core region partly results from the size matching between the Mn and Zn atoms. In the core position, the magnetic moment of the Mn ion is calculated to be 4.88  $\mu_B$ , in good agreement with other calculated values of 4.6 and 4.89  $\mu_B$ .<sup>23,29</sup> The crystal field splitting of the Mn  $3d$  states into the  $e_g$  and  $t_a$  states is 0.80 eV [Fig. 2(a)], similar to the result for bulk (Zn,Mn)O.<sup>16,22,23</sup> Due to the trigonal symmetry, the  $t_a$  levels further split into a singlet and a doublet level. For the  $e_g$  and  $t_a$  states, the exchange splittings are estimated to be 3.31 and 2.81 eV, respectively, in the LSDA, much larger than the crystal field splitting, while these values increase by 2.3 eV in the LSDA+ $U$ .

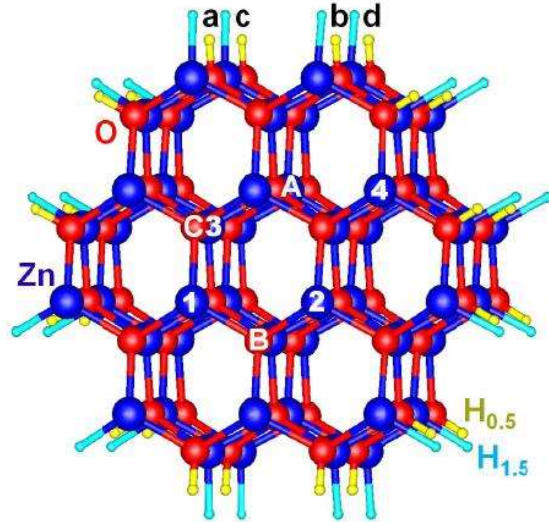


**Fig. 1.** A supercell geometry of the [0001] ZnO nanowire, in which the surface atoms are passivated by pseudo-H atoms with 0.5 and 1.5 electrons. Blue and red balls represent the Zn and O atoms, respectively. Possible positions of defects are labeled by a, b, c, and d for the surface O dangling bonds, by 1, 2, and 3 for the Mn ions.

Next we investigate the magnetic coupling between the Mn ions in ZnO NWs. As the Mn

ions prefer to occupy the inner sites, we consider several Mn configurations in which two Mn ions are positioned in the core region. In configurations I and II, each Mn pair consists of two neighboring Mn ions at the sites 1 and 2 on the basal plane or the sites 1 and 3 along the wire axis (Fig. 1). Due to the hexagonal symmetry, these two configurations are crystallographically different from each other. In the wire structure, relaxations slightly elongate the wire and reduce the diameter. Thus, the Mn-Mn distance (3.039 Å) of the Mn pair on the basal plane is shorter than that (3.250 Å) along the wire axis (Table I). In configuration III, the Mn ions occupy the sites 1 and 4 which are far from each other, with the distance of 5.341 Å. The energy differences ( $\Delta E_{\text{AFM-FM}}$ ) between the AFM and FM states are compared for three configurations in Table I. In configurations I and II, the AFM state is found to be energetically more stable by 89 and 46 meV, respectively, than the FM one, while  $\Delta E_{\text{AFM-FM}}$  is -51 meV for the Mn pair on the basal plane in bulk (Zn,Mn)O, similar to other calculations.<sup>20</sup> In configuration III,  $\Delta E_{\text{AFM-FM}}$  is nearly zero, indicating that a paramagnetic ordering is more favorable. This result also infers that the magnetic coupling between the Mn ions has the short-range nature. The most stable configuration of two Mn ions is the AFM state of configuration I, which is lower in energy by 61 meV than that of configuration II. Our results are consistent with previous calculations for bulk (Zn,Mn)O and Mn-doped ZnO NWs.<sup>21,29</sup> In the LSDA+*U* calculations, the stability of the AFM state against the FM one is reduced by 0.15 and 0.10 eV for the configurations I and II, respectively, as compared to the LSDA results.<sup>29</sup>

The density of states and the projected density of states onto the Mn ion are shown in Fig. 2(b). The AFM state exhibits the narrow majority  $t_a$  states than for the FM state. As the  $t_a$  states are fully occupied, the AFM state becomes stabilized due to the energy gain by the superexchange coupling, while there is no energy gain in the FM coupling. In bulk (Zn,Co)O, it was suggested that the magnetic state changes from antiferromagnetic to ferromagnetic if the minority  $t_a$  states are partially occupied by additional electron doping.<sup>12</sup> In the (Zn,Mn)O NW, as the minority  $e_g$  and  $t_a$  states lie well above the conduction band minimum [Fig. 2(b)], it is difficult to populate these states by additional electron doping. Even if the electron carrier density reaches  $8.75 \times 10^{20} \text{ cm}^{-3}$ , the stability of the AFM state remains unchanged, with  $\Delta E_{\text{AFM-FM}} = -90 \text{ meV}$ , in contrast to previous LSDA calculations.<sup>29</sup>

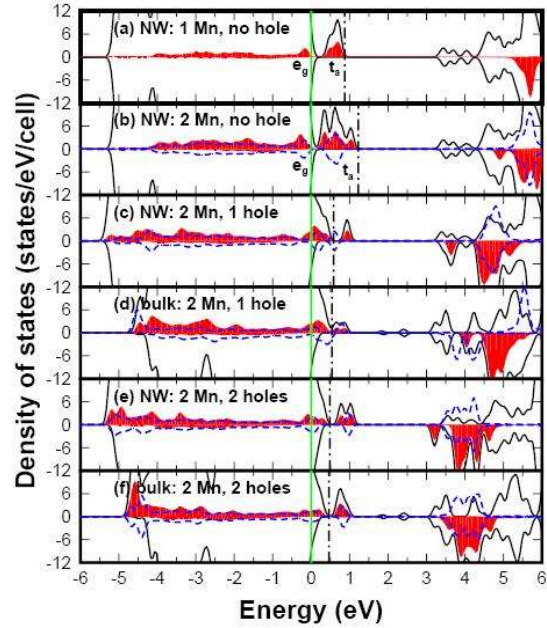


**Fig. 2.** The total densities of states (black solid lines in the FM state) and the projected density of states (red shaded areas in the FM state whereas blue dashed lines in the AFM state) onto the Mn ions are compared for (a)-(b) carrier-free ZnO NWs with one and two Mn ions in the supercell, respectively, and (c)-(f) bulk (Zn,Mn)O and Mn-doped ZnO NWs with one or two additional hole carriers. Vertical green solid and black dot-dashed lines denote the VBM and the Fermi level, respectively, for the FM state.

On the other hand, many theoretical and experimental studies showed that bulk (Zn,Mn)O becomes ferromagnetic with additional hole doping.<sup>10-12,15-23</sup> To examine the effect of additional hole doping on the ferromagnetism of (Zn,Mn)O NWs, we consider two different doping strategies, in which hole carriers are generated by simply adding hole carriers, by introducing Zn and O dangling bonds (DBs) on the surface. For the Mn ions in the stable configuration I, the results for the stability of the FM state against the AFM one are compared in Table II. In general, the FM state becomes stabilized by additional *p*-type doping. We find that hole carriers are mostly localized in the majority  $t_a$  states, lowering the Fermi level. For the carrier density of one hole per Mn-Mn pair, the O atoms adjacent to the Mn ions undergo large relaxations of about 0.12 Å. In addition, due to symmetry breaking relaxations, the majority  $t_a$  states split into two groups, the empty and occupied states, and they become broadened. We find that the positions of the empty  $t_a$  states in the FM state are higher by 0.05 and 0.33 eV than those for the AFM state in bulk and nanowire systems, respectively [Figs. 2(c) and

2(d)]. Due to the localized holes, the FM state becomes stabilized via the double exchange interaction, with the energy difference  $\Delta E_{\text{AFM-FM}} = 140$  meV, similar to the bulk value of 154 meV. When two holes per Mn-Mn pair are doped in the

NW, the empty  $t_a$  states are broadened, with two peaks separated by about 0.25 eV, while no splitting occurs for bulk (Zn,Mn)O [Figs. 2(e) and 2(f)]. The FM coupling is much weakened, with  $\Delta E_{\text{AFM-FM}} = 14$  meV.

**Table I.** For various configurations of two Mn ions in ZnO nanowire, the energy differences ( $\Delta E_{\text{AFM-FM}}$  in eV) between the AFM and FM states, the stable spin configurations, the Mn-Mn distances ( $d_{\text{Mn-Mn}}$  in Å), and the magnetic moments ( $m$  in  $\mu_B$ ) of the Mn ions are compared. The third column represents the energies ( $\delta E$  in eV) relative to the most stable configuration. Numbers in the first column denote the Zn sites in Fig. 1.

Configuration of two Mn ions	$\Delta E_{\text{AFM-FM}}$	$\delta E$	Spin state	$d_{\text{Mn-Mn}}$	$m(\text{Mn}_1)$	$m(\text{Mn}_2)$
I(1,2)	-0.089	0.000	AFM	3.039	4.561	-4.561
II(1,3)	-0.046	0.061	AFM	3.250	4.571	-4.572
III(1,4)	0.000	0.082	Para	5.341	4.585	4.603

**Table II.** For various hole-doping strategies in Mn-doped ZnO nanowire, the energy differences ( $\Delta E_{\text{AFM-FM}}$  in eV) between the AFM and FM states, the stable spin states, the Mn-Mn distances ( $d_{\text{Mn-Mn}}$  in Å), and the total magnetic moments ( $m_{\text{tot}}$  in  $\mu_B$ ) are compared. Numbers in parentheses represent the results for bulk (Zn,Mn)O.

	$\Delta E_{\text{AFM-FM}}$	Spin state	$d_{\text{Mn-Mn}}$	$m_{\text{tot}}$
Additional hole carrier				
one hole	0.140(0.154)	FM	3.0361	8.84(8.80)
two holes	0.014(0.019)	FM	3.1447	7.90(7.86)
Surface oxygen DB				
one DB	0.042	FM	3.0890	9.30
two DBs	0.123	FM	3.0494	8.84
three DBs	0.150	FM	3.0360	9.31
four DBs	0.093	FM	3.0466	9.79

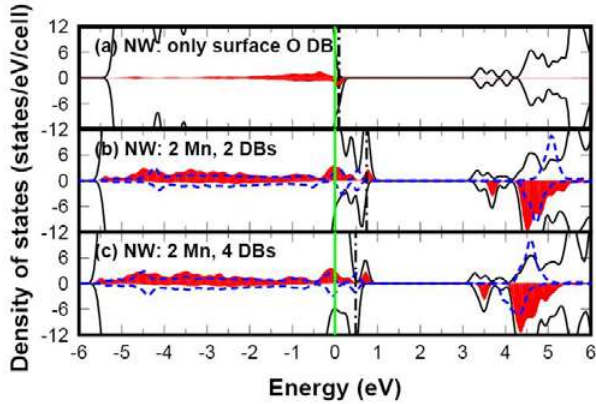


**Fig. 3.** The total densities of states (black solid lines in the FM state) and the projected density of states (red shaded areas in the FM state whereas blue dashed lines in the AFM state) onto the Mn ions are compared for (a) Mn-free ZnO NW with only one surface O DB and (b)-(c) Mn-doped ZnO NWs with two and four surface O DBs, respectively. Vertical green solid and black dot-dashed lines denote the VBM and the Fermi level, respectively, for the FM state.

Surface oxygen DBs act as an acceptor, generating 0.5 holes per DB defect. We introduce up to four surface oxygen DBs by removing pseudo-H atoms labeled *a*, *b*, *c*, and *d* in Fig. 1. As the surface DBs are separated by 5.54–6.25 Å from the Mn ions, structural relaxations do not

affect significantly the magnetic coupling between the Mn ions. For all configurations with different numbers of the surface DBs, we find that the FM state is more stable than the AFM one (Table II). As the number of the surface DBs increases from one to two,  $\Delta E_{\text{AFM-FM}}$  increases rapidly from 0.042 to 0.123 eV, which is close to the energy difference of 0.140 eV for one additional hole case. In the (Zn,Mn)O NW, the defect levels of the surface oxygen DBs are located slightly below the majority  $t_a$  levels, as shown in Fig. 3. Thus, a charge transfer occurs from the Mn ions to the DBs, inducing hole carriers in the  $t_a$  levels. The hole carriers are estimated to be 0.50 and 0.93 holes for one and two DBs, respectively. Actually, an isolated surface DB in Mn-free ZnO NW has the intrinsic magnetic moment of 0.48  $\mu_B$  [Fig. 3(a)]. However, for three and four DBs, an incomplete charge transfer occurs due to the proximity of the DB levels to the majority  $t_a$  states. The doping level of the majority  $t_a$  levels is found to saturate to about one hole per Mn-Mn pair, while extra hole carriers are distributed at the DB defects [Figs. 3(b) and 3(c)]. When four DBs are introduced, the total magnetic moment increases to 9.79  $\mu_B$  due to the contributions from the DB states, as compared to the magnetic moment of

8.84  $\mu_B$  for two DBs. On the other hand, the ferromagnetic coupling is slightly weakened, with  $\Delta E_{AFM-FM} = 93$  meV.

#### IV. CONCLUSION

In conclusion, we have studied the hole-carrier-mediated ferromagnetism of Mn-doped ZnO nanowires through the first-principles calculations within the LSDA+ $U$  approach. While the ground state of carrier-free (Zn,Mn)O NWs is the antiferromagnetic state, the ferromagnetism is promoted by additional  $p$ -type doping, which induces localized holes in the majority  $t_a$  levels of the Mn ions. For various  $p$ -type doping strategies, (Zn,Mn)O NWs exhibit a tendency that the maximum stability of the ferromagnetic state occurs for the doping level of about one hole per Mn-Mn pair. For the surface oxygen DB defects, the number of transferred charges from the majority  $t_a$  levels to the DB states saturates to one hole per Mn-Mn pair due to the proximity of the acceptor level to the  $t_a$  levels.

#### Acknowledgments

This work was supported by National Research Foundation of Korea under Grant No. NRF-2009-0093845 and the BK21 Project.

#### REFERENCES

1. H. Ohno, Science 281 (1998) 951.
2. T. Dietl, H. Ohno, F. Matsukura, J. Cibert, D. Ferrand, Science 287 (2000) 1019.
3. K. Nomura, H. Ohta, K. Ueda, T. Kamiya, M. Hirano, H. Hosono, Science 300 (2003) 1269.
4. D.C. Look, Mater. Sci. Eng. B 80 (2001) 383.
5. A. Tiwari, C. Jin, A. Kvit, D. Kumar, J.F. Muth, J. Narayan, Solid State Commun. 121 (2002) 371.
6. T. Fukumura, Z. Jin, M. Kawasaki, T. Shono, T. Hasegawa, S. Koshihara, H. Koinuma, Appl. Phys. Lett. 78 (2001) 958.
7. S.W. Jung, S.-J. An, G.-C. Yi, C.U. Jung, S.-I. Lee, S. Cho, Appl. Phys. Lett. 80 (2002) 4561.
8. P. Sharma, A. Gupta, K.V. Rao, F.J. Owens, R. Sharma, R. Ahuja, J.M.O. Guillen, B. Johansson, G.A. Gehring, Nature Mater. 2 (2003) 673.
9. W. Yan, Z. Sun, Q. Liu, Z. Li, Z. Pan, J. Wang, S. Wei, D. Wang, Y. Zhou, X. Zhang, Appl. Phys. Lett. 91 (2007) 062113.
10. Q. Xu, H. Schmidt, L. Hartmann, H. Hochmuth, M. Lorenz, A. Setzer, P. Esquinazi, C. Meinecke, M. Grundmann, Appl. Phys. Lett. 91 (2007) 092503.
11. H.Y. Xu, Y.C. Liu, C.S. Xu, Y.X. Liu, C.L. Shao, R. Mu, Appl. Phys. Lett. 88 (2006) 242502.
12. K. Sato, H. Katayama-Yoshida, Jpn. J. Appl. Phys., Part 2 39 (2000) L555; *ibid.*, 40 (2001) L334; Semicond. Sci. Technol. 17 (2002) 367; Phys. Status Solidi B 229 (2002) 673.
13. G.M. Dalpian, S.-H. Wei, X.G. Gong, A.J.R. da Silva, A. Fazzio, Solid State Commun. 138 (2006) 353.
14. G.M. Dalpian, S.-H. Wei, Phys. Status Solidi B 243 (2006) 2170.
15. Q. Wang, Q. Sun, P. Jena, Y. Kawazoe, Phys. Rev. B 70 (2004) 052408.
16. D. Maoche, P. Ruterana, L. Louail, Phys. Lett. A 365 (2007) 231.
17. O. Mounkachi, A. Benyoussef, A. El Kenz, E.H. Saidi, E.K. Hlil, J. Magn. Magn. Mater. 320 (2008) 2760.
18. Y. Zhu, J.X. Cao, Z.Q. Yang, R.Q. Wu, Phys. Rev. B 79 (2009) 085206.
19. M.H.F. Sluiter, Y. Kawazoe, P. Sharma, A. Inoue, A.R. Raju, C. Rout, U.V. Waghmare, Phys. Rev. Lett. 94 (2005) 187204.
20. P. Gopal, N.A. Spaldin, Phys. Rev. B 74 (2006) 094418.
21. D. Iușan, B. Sanyal, O. Eriksson, Phys. Rev. B 74 (2006) 235208.
22. N.A. Spaldin, Phys. Rev. B 69 (2004) 125201.
23. T. Chanier, M. Sargolzaei, I. Opahle, R. Hayn, K. Koepf, Phys. Rev. B 73 (2006) 134418.
24. H.-W. Zhang, E.-W. Shi, Z.Z. Chen, X.-C. Liu, B. Xiao, Jpn. J. Appl. Phys., Part 1 45 (2006) 7688.
25. S. Deka, P.A. Joy, Solid State Commun. 142 (2007) 190.
26. J.J. Liu, M.H. Yu, W.L. Zhou, Appl. Phys. Lett. 87 (2005) 172505.
27. U. Philipose, S.V. Nair, S. Trudel, C.F. de Souza, S. Aouba, R.H. Hill, H.E. Ruda, Appl. Phys. Lett. 88 (2006) 263101.
28. H.L. Yan, X.L. Zhong, J.B. Wang, G.J. Huang, S.L. Ding, G.C. Zhou, Y.C. Zhou, Appl. Phys. Lett. 90 (2007) 082503.
29. H. Shi, Y. Duan, J. Appl. Phys. 103 (2008) 073903.
30. Q. Wang, Q. Sun, G. Chen, Y. Kawazoe, P. Jena, Phys. Rev. B 77 (2008) 205411.
31. G. Kresse, J. Furthmüller, Phys. Rev. B 54 (1996) 11169; *ibid.*, 59 (1999) 1758.
32. J.J. Monkhorst, H.J. Pack, Phys. Rev. B 13 (1976) 5188.
33. R.A. Powell, W.E. Spicer, J.C. McMenamin, Phys. Rev. Lett. 27 (1971) 97; C.J. Vesely, R.L. Hengehold, D.W. Langer, Phys. Rev. B 5 (1972) 2296; G. Zwicker, J. Jacobi, Solid State Commun. 54 (1985) 701.

34. T. Mizokawa, T. Nambu, A. Fujimori, T. Fukumura, M. Kawasaki, Phys. Rev. B 65 (2002) 085209; F. Bondino, K.B. Garg, E. Magnano, E. Carleschi, M. Heinonen, R.K. Singhal, S.K. Gaur, F. Parmigiani, J. Phys.: Condens. Matter 20 (2008) 275205.
35. B.D. Yuhas, S. Fakra, M.A. Marcus, P. Yang, Nano Lett. 7 (2007) 905.
36. X. Zhang, Y. Zhang, Z.L. Wang, W. Mai, Y. Gu, W. Chu, Z. Wu, Appl. Phys. Lett. 92 (2008) 162102.
37. C.H. Park, S.B. Zhang, S.H. Wei, Phys. Rev. B 66 (2002) 073202.